

PUZZLE TASK ERP RESPONSE: TIME-FREQUENCY AND SOURCE LOCALIZATION ANALYSIS

Ahmed Almurshedi^{1,2*}
Abd Khamim Ismail¹

¹Department of Physics, Faculty of Science, Universiti Teknologi Malaysia (UTM), 81310, Skudai, Johor, Malaysia
²Physics Department, College of Science, Al-Muthanna University (IRAQ)

Abstract

Perceptual decision making depends on the choices available for the presented task. Most event-related potential (ERP) experiments are designed with two options, such as YES or NO. In some cases, however, subjects may become confused about the presented task in such a way that they cannot provide a behavioral response. This study aims to put subjects into such a puzzled state in order to address the following questions: How does the brain respond during puzzling moments? And what is the brain's response to a non-answerable task? To address these questions, ERP were acquired from the brain during a scintillation grid illusion task. The subjects were required to count the number of illusory dots, a task that was impossible to perform. The results showed the presence of N130 over the parietal area during the puzzling task. Coherency among the brain hemispheres was enhanced with the complexity of the task. The neural generators' source localizations were projected to a multimodal complex covering the left postcentral gyrus, supramarginal gyrus, and angular gyrus. This study concludes that the brain component N130 is strongly related to perception in a puzzling task network but not the visual processing network.

Keywords

• Puzzled response • Decision making • Event-related potential (ERP) • Scintillation grid illusion
• N130 • Time-frequency analysis • Source localization analysis • Measure projection analysis

Received 12 May 2015
accepted 28 August 2015

1. INTRODUCTION

Human brain perceptions have been the focus of many recent electrophysiological studies. Numerous studies have looked at perceptual and cognitive functions such as selective attention [1] and decision making [2]. Perceptual decision making has recently attracted the interest of many researchers of non-pathological brain processing, which provide a better understanding of brain mechanisms and networks. Experimental studies have focused on characterizing the temporal evolution of component activities, which is correlated with perceptual decision making, and on quantifying the relationship between neural signals and the behavioral response by comparing neurometric and psychometric functions [3]. Studies have raised questions regarding the difficulty of decision making and its relationship with the allocation of the neural timing resources in cortical processing. These studies also discuss how the difficulty of the decision relates to decision accuracy [4]. The decision-related area of the brain was identified by combining the high temporal resolution


of electroencephalography (EEG) with the high spatial resolution of functional magnetic resonance imaging (fMRI) [5].

Temporal analysis of EEG relies mainly on brain response event-related potentials (ERP). Several investigators have preferred the use of visual illusion tasks in their experiments. For instance, the Craik Cornsweet O'Brien (CCOB) illusion is used to study the sensitivity of the visual mismatch negativity (vMMN) with the oddball paradigm [6]. One comparative study investigated the cortical response to the cue paradigm using the face-vase illusion figure [7]. The study attributes the appearance of early N100 and late N320 to the deployment of attention (conscious effort) in the selection of the target and to involuntary perceptual reversals, respectively. Some researchers have used the Thatcher illusion for face and object processing and have observed a disruption in brain perception caused by the illusion. A higher density of brain potentials were also noted as a result of illusion characterization [8, 9]. One study used the composite face effect (CFE) illusion aimed at encoding facial images and found an increasing N170 response

over the occipital temporal area [10]. Other studies have used semantic illusion tasks such the use of illusory words [11], and language processing with a semantic illusion task [12, 13]. The Kanizsa squares illusion task has been widely used to study different temporal brain perceptions. Such studies use this type of illusion with magnetoencephalography (MEG) [14], with progressive misalignment of Kanizsa figures [15], in investigating temporal and spatial attention binding with different orders of figures [16] and in clinical procedures for autism at high and low frequencies [17-19].

Source localization dipole fitting of ERP have been employed with some kinds of illusion tasks. For instance, the Müller-Lyer illusion was used to investigate ERP and estimate the dipole sources, with the result indicating that the anterior cingulate cortex (ACC) might contribute to the illusion effect [20]. The McGurk illusion was used to investigate MMN and study source localization. The results were mostly distributed on the lateralized left hemisphere, giving a response at 175 ms. The dipole source analysis showed that the sources were mostly related to the left temporal gyrus.

* E-mail: fhahmed2@gmail.com

 © 2015 Ahmed Almurshedi, Abd Khamim Ismail, licensee De Gruyter Open.

This work is licensed under the Creative Commons Attribution-NonCommercial-NoDerivs 3.0 License.

Thus, the left temporal cortex plays a vital role in this type of illusion process [21].

As seen above, visual illusion tasks have occasionally been used in the research on brain perceptions. Illusions are usually described as visual images that differ from reality, where the eyes and the brain perceive something that does not exactly match the physical measurements of the displayed image. Through exaggerated attention, the eyes and brain make unconscious inferences. Even when the brain knows the presented task is an illusion, the error still occurs. Hence, the brain cannot help perceptually with countering this effect. This clearly shows that brain perception carries with it a certain amount of misreading. The nervous system processes and approximates visual information mainly based on color, shape, and dimension. To address this issue, this paper provides a comprehensive study of the visual evoked potentials (VEP) modified by the scintillation grid illusion to study brain perception and the brain response evoked by a puzzling task (inability to make a decision) in different age groups. This result was then used to do a time-frequency analysis and study the cross coherence between brain hemispheres. Furthermore, measure projection analysis (MPA) was discussed to anatomically localize the source generator in the brain domain.

2. MATERIALS AND METHODS

2.1 Subjects

Thirty-four male subjects volunteered for this experiment and signed the informed consent form. According to Van den Bos *et al.* [22], performance differences exist between males and females. Males tend to focus exclusively on long-term goals while females tend to balance short and long-term interests. In other words, males shift from exploration to exploitation, while females remain exploratory. These differences were explained as possibility being due to differences in the general dynamics of neurotransmitter systems, that is, differences in brain serotonergic and dopaminergic activity [22]. As such, only male subjects were included in the present study. Subjects were healthy, with no history of neurological, psychological and ophthalmological diseases. They were

divided into two age groups: the young group (16 subjects), with an average age of 10.8 ± 2.6 (mean \pm SD) years old and the mature group (18 subjects), all of whom were postgraduate students with an average age of 25 ± 2.6 years old. Most of the subjects were right handed and all had normal or corrected-to-normal visual acuity, tested with a Snellen chart. Some of the subjects wore corrective lenses during the experiment. The subjects were informed about the protocol and the aim of this study. They were instructed to sit comfortably on a chair placed at a fixed distance (100 cm) from the monitor and to try to avoid any physical movements such as head or body movements, blinking, yawning or biting to prevent unwanted muscular artifacts in the useful EEG signal. They were also asked to maintain their attention during the experiment.

2.2 Stimulation tasks

The experiment included the combined task of VEP pattern reversal checkerboard stimulation with a scintillation grid illusion picture, as shown in Fig. 1. The visual stimulation pattern was first designed using Delphi programming language following the International Society for Clinical Electrophysiology of Vision (ISCEV) standard [23]. It was then modified and combined with a scintillation grid illusion picture, which was displayed at the center of the pattern reversal stimulation.

In the stimulation task, the subjects were required to count the number of black dots in the illusion, something that could not be counted. The purpose was to analyze and extract the brain's response to the confusing task, which was called the puzzled task. The task was the modified version of the pattern reversal checkerboard, which is standard stimulation used for VEP recording. The pattern reversal checkerboard stimulation consisted of black and white checks displayed on a full screen. Visual stimulation software was designed for precise stimulation of the brain, with adjustable parameters such as the number of horizontal and/or vertical checks (spatial resolution). The checks were reversed at the specific frequency of 1 Hz (the black check turns white and then back to black in one second), as shown in Fig 1. The duration of data recording was 100 sec, with a total 200 trials from each subject.

In the grid illusion, black dots appear and vanish at the junctions between the grey lines of the grid. Directing attention to a single white dot in the picture creates the illusion of black dots appearing at the opposite side of the point of attention. This effect increases when the eyes scan across the illusion picture, with dense black dots appearing. With the head angled at 45° , the effect is slightly reduced, but not eliminated. The effect seems to exist only at intermediate distances (of about 3-5 feet, i.e. 90-150 cm) from the object. This effect may

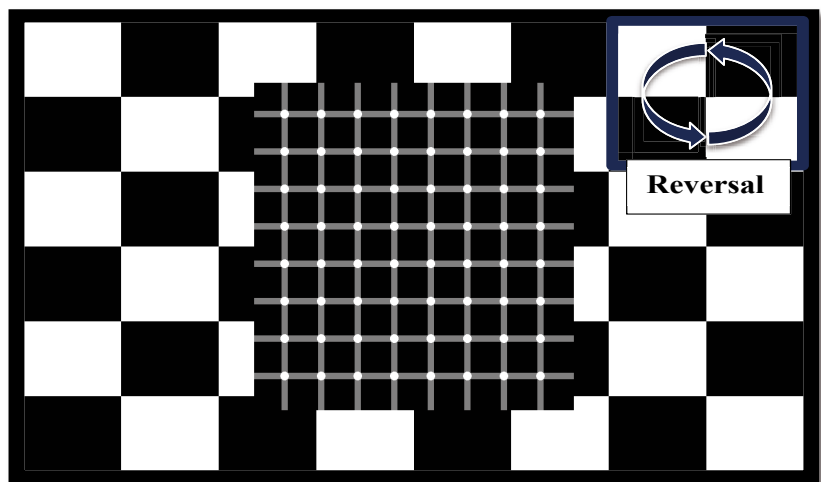


Figure 1. Experimental task performance. Pattern reversal checkerboard visual evoked potential stimulation, modified using a scintillation grid illusion to extract the puzzled response. The subjects were asked to count the number of illusory dots in the illusion.

be explained by a neural process called visual lateral inhibition. In this process, photoreceptor cells aid the brain in perceiving contrast within the picture, while another group of receptor cells respond to the appearance of stimuli [24].

The illusion picture (image size: 494 x 404 pixels, 24 bits/pixel) was fixed at the center of the screen and the pattern reversal checkerboard was maintained, as shown in Fig. 1. The grid illusion picture was used, and the subjects were required to count the number of illusory black dots (target) in the central picture. They were instructed to try to make a decision about the number of black dots, if they could. This could include unreal dots appearing due to the high contrast between edges of the white and black colors. This experiment was designed to catch the subjects' attention, keep them mindful during the experiment, and to increase the complexity of the task.

2.3 Data acquisition

A standardized recording scheme was developed; every subject was to perform the tasks in a fixed and repetitive pattern, according to the scheme on the monitor screen. EEG data was collected using 24 channels on the Contec KT88-2400 data acquisition system (Contec Medical Systems, Qinhuangdao, China) in a dim, electrically and acoustically shielded room. The impedance of each electrode was tested with the help of a light emitting diode (LED) indicator on the EEG machine, which lit up when the impedance exceeded 5 K Ω . Bridge dry electrodes were distributed over entire scalp following the 10-20 electrode system. The electrodes on each hemisphere were referenced to the appropriate earlobe (right and left) with a forehead ground. The recorded data was re-referenced to the average reference of all electrodes during post-processing. A net head cap was used to fix the electrodes at their positions. The data was digitized at 200 Hz sampling frequency, with all unwanted frequencies filtered out using a 0.1-35 Hz bandpass filter. The EEG data was recorded in a time-locked manner to the reversal pattern of checkerboard and the trigger marker was detected by a photo sensor attached to the screen. The recording system was calibrated and synchronized to the stimulation task.

2.4 Data analysis

Grand average brain responses were extracted by time-locked average of multiple subjects and trials of pattern stimulation. Background EEG and other sources of noise were distributed randomly along the recorded signal. Averaging of the trials was done to increase the signal to noise ratio (SNR) of the recorded ERP.

If K is the trial number ($K=1,2,\dots,N$) and t is the time of single trial, the recorded response can be described as:

$$\bar{x}(t) = \frac{1}{N} \sum_{k=1}^N x(t, k) = s(t) + \frac{1}{N} \sum_{k=1}^N n(t, k) \quad (1)$$

Where, $s(t)$ is the signal and $n(t,k)$ is the random noise. It was noticed that the noise is not correlated with the trial number, while the signal is.

Visual inspection is used for artifact removal from the continuous EEG data prior to time-locked averaging. Independent component analysis (ICA) is used for automatic correction of artifacts and epoch rejection following the time-locked averaging to eliminate noise from the recorded data [25].

In order to perform time-frequency analysis, event-related spectral perturbation (ERSP) is required to compute a power spectrum over a sliding time window across data trials [25]. ERSP visualizes mean event-related changes in spectral power over time in a broad frequency range. The color (blue to red) on each pixel of the time-frequency analysis image indicates the power (in dB) at a given frequency and latency relative to the time-locked event. This representation shows the relationship between the three variables of time, frequency, and power spectrum. For instance, the higher power spectrum may be marked with a red color, and this power can be seen at a specific time t from the onset of the stimulation, and this is presented with a specific of frequency range f of the brain response. Typically, if $F_k(f,t)$ is the spectral estimate of trial number ($K=1,2,\dots,N$) at frequency f and time t :

$$ERSP(f, t) = \frac{1}{N} \sum_{k=1}^N |F_k(f, t)|^2 \quad (2)$$

In Equation 2, $F_k(f, t)$ is a sinusoidal wavelet transform, which provides a specified time and frequency resolution.

Time-frequency decomposition in EEGLAB (an interactive Matlab open source environment for processing of electrophysiological signal data, Matworks Inc., Natick, MA, USA) is based on multi-taper analysis and a single type of sinusoidal wavelet, as is standard for EEG analysis. Quantitative comparisons show that the results of EEG data using other methods, such as Hilbert transforms, do not differ dramatically from applying sinusoidal wavelets [26]. Sinusoidal wavelets with a number of cycles increase slowly with frequency, although the number of cycles in each data window can be critical. This feature allows a better frequency resolution to be obtained at higher frequencies than a conventional wavelet approach, which uses a constant cycle length. To visualize power changes across the frequency range, the mean baseline log power spectrum is subtracted from each spectral estimate, producing the baseline normalized ERSP [25].

Cross coherence is the phase stability between two different time series that combines the phase angle between them. The magnitude of cross coherence is either 1, if the phase difference between signals is constant (perfect phase synchronization) or 0, if the phase difference between signals is random (absence of phase synchronization) at a given time t and frequency f . In certain cases, a constant phase difference appears between two different frequencies. This is termed cross frequency coherence or bi-spectral coherence [27, 28]. Coherence is essential because the degree of relationship or coupling between any two living systems cannot be fully understood without knowledge of their frequency structure over a relatively long period of time.

Cross coherence between hemispheres of the brain can be determined by computing the event-related potential coherence (ERPCOH) between two relative channels of EEG [25]. For any two signals, a and b , phase cross coherence is defined by Equation 3, where $F_k^b(f, t)^*$ is the complex conjugate of $F_k^b(f, t)$.

$$ERPCOH^{a,b}(f, t) = \frac{1}{N} \sum_{k=1}^N \frac{F_k^a(f, t) F_k^b(f, t)^*}{|F_k^a(f, t) F_k^b(f, t)|} \quad (3)$$

To estimate the sources of the recorded signal in the brain and localize them to different

domains, measure projection analysis (MPA) method was used. This method statistically characterizes the spatial consistency of EEG dynamics across a set of data by combining the information across a large number of subjects, each of whom is associated with his or her own set of source processes and scalp projections [29]. This method has been used in the first application of MPA to EEG datasets collected in a visual task and decomposed separately using extended infomax ICA (independent component analysis) [30]. An infomax ICA is an unsupervised nonlinear learning algorithm based on an information maximization network. Its application to an ensemble of natural scenes produces sets of visual filters that are localized and oriented. In addition, the outputs of these filters are as independent as possible, since the infomax network performs ICA for sparse (super-Gaussian) component distributions [31].

MPA provides statistically significant values with fewer parameters compared to other clustering methods. Bigdely-Shamlo *et al.* [29] applied MPA to surrogate data derived from rapid visual serial presentation (RVSP) tasks, obtaining results that were not highly sensitive to prior parameter choices.

MPA was begun by computing the location of each source of an independent component resulting from ICA decomposition. It was performed on the brain template model in the form of an equivalent dipole source. Subsequently, dipole locations of dipoles were smoothed using a 3-D Gaussian spatial kernel model. Similarities between local independent components were measured in the subspace of brain voxels locations. Finally, affinity clustering was used to identify brain domains with sufficient differences in the brain subspace [29]. Measure Projection Toolbox (an extension to EEGLAB) allows the user to graphically display the domains in different patterns. It also produces a summary of anatomical locations associated with Brodmann's areas.

After the ICA decomposition, the components were accurately modeled by an equivalent dipole $D(x)$ located at any brain location $x \in V \subset R^3$. Then the dipoles were clustered with the MPA method. In MPA clustering, consider a measure vector as $M(x)$,

which is obtained by vectorizing ERP or ERSP, associated with an IC and equivalent dipole $D(x)$. Measured vectors typically estimate mean event-related changes in IC source activity, which are related to the change in recorded scalp potential. In an ERP study, n IC processes associated with n distinct equivalent dipoles $D_i = D(x_i)$ (with indices $x_i, i=1, \dots, n$) may be active.

For an arbitrary brain location $y \in V$, the expected (projected) value for the interpolated measure vector $M(y)$ is

$$E\{M(y)\} = \langle M(y) \rangle = \frac{\sum_{i=1}^n P_i(y) M_i}{\sum_{i=1}^n P_i(y)} \quad (4)$$

$P_i(y)$ is the probability, given by

$$P_j(y) = TN(y; \hat{x}_j, \sigma^2, l, \epsilon) \quad (5)$$

where σ is the standard deviation of a spherical 3-D multivariate Gaussian with covariance σ^2 . l is centered at an estimated dipole D_j location \hat{x}_j and TN is a normalized truncated Gaussian distribution. Since the probabilities must sum to one ($\sum_{i=1}^n \bar{P}_i = 1$), it is natural to define as in Equation 6, which shows that our estimate is given by a convex combination (weighted average) of measure values M_i that depends on equivalent dipole location $y \in V$.

$$\bar{P}_i(y) \equiv \frac{P_i(y)}{\sum_{i=1}^n P_i(y)} \quad (6)$$

We wanted to estimate an interpolated measure vector $M(y)$, that is, an estimate of the measure vector across each possible brain voxel location, and to estimate the statistical significance (p-value) of this assignment at each of these locations. The probability distribution of projected measures $M(y)$ is performed under the null hypothesis. The estimated measure vector is actually produced by a random spatial distribution in the brain and there is no significant similarity between these vectors within neighborhoods centered at brain locations $y \in V$. This is necessary to be able to assign any statistical meaning to the projected values [29].

3. Results and discussion

To explore brain responses related to the tasks presented in Fig. 1, the grand average of different age groups was calculated. The

illusion task was presented and the brain response extracted during puzzling moments.

Pattern reversal VEP using checkerboard stimulation is a well known response. The P100 exhibits a prominent peak of VEP, which indicates little variation between subjects and little within subject interocular difference, with repeated measurements over time [23]. VEP was used here as a reference signal for the modified combination task of the scintillation grid illusion.

The experiment was focused on the illusion task and purposely designed to put the subjects into a situation in which they could not answer the question presented by the task (i.e. they would be unable to make a decision). The subjects were asked to count the number of black dots, a task that is impossible. In order to extract brain response from background noise, a time-locked grand average was calculated on all channels.

3.1 Illusion component N130

A scintillation grid illusion was used in the task. The subjects were required to count the number of black dots that only appeared to exist but in reality, did not. The stimulation background contained the black and white pattern reversal checkerboard to limit the specific time window, and the ERP from this combination (grid illusion and pattern VEP) were extracted. The task was chosen in order to keep the subjects' attention and to present them with a decision that was an impossible task.

In the presented task, the grand average of the illusion task indicated activation the parietal area of brain. As shown in Fig. 2(a), a negative response appeared in the parietal lobe, with a fixed latency of around 130 ms (its maximum value never reached 150 ms) from the onset of the checkerboard stimulation. Since the illusion task stimulates the neural cognitive network of the brain, the N130 response might be a representation of the confusion response. However, the response was clearly seen in the middle, left and right parietal electrodes. It is also important to mention the presence of small peak responses P80 and P200. These peaks were seen mostly in the parietal area.

The reliability of N130 across the subjects (trials) was plotted over latency, as shown in

Fig. 2(b). The ERP image is consistent over the first 10 trials, as recorded from the parietal area. The plotted brain topography scalp map of N130 shows growth in the parietal lobe of the brain. The topography presented in Fig. 2(c) represents the power distribution over the entire scalp, but cannot clearly separate between brain regions due to the combination

task (visual and perceptual stimulation) and the interference between electrodes. Generally, few ERP studies have reported such a presence of N130 response. As the literature provides no confirmation about what N130 actually represents, it remains an arguable point. Most of the research indicates that N130 is the first negative peak appearing after the

onset of external stimulation. It was previously called N1, where N refers to the negative polarity and 1 indicates the first negative peak after the onset. N1 components have been reported with latencies lying between 150-200 ms for different task conditions [7, 32-34]. Among recent ERP studies utilizing the visual illusion task, very few (as summarized in Table

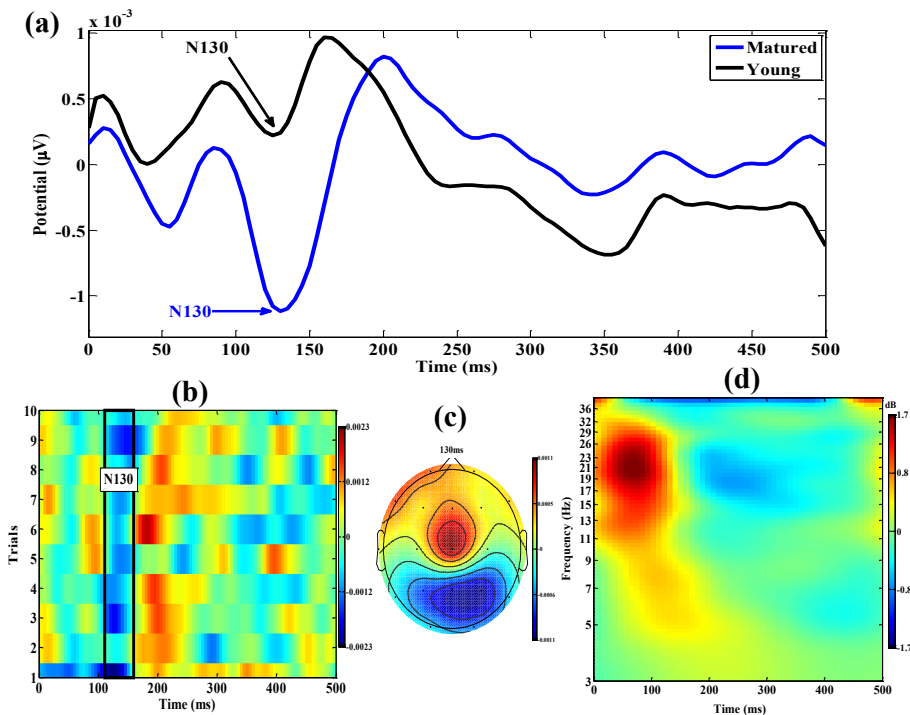


Figure 2. Illusion task analysis representation. (a) Grand average puzzled response resulting from the illusion task stimulation on the middle parietal electrode (Pz). The N130 response appears 130 ms after the onset of the stimulation task. Higher N130 amplitude is found in the mature (blue curve) age group, as compared to the young (black curve) age group. (b) Consistency of the first 10 trials with time. In all the trials, the N130 response is found at the same latency following the stimulation onset. (c) Brain topography scalp map. The negativity at 130 ms of power spectral is concentrated at the posterior part of the scalp. (d) Time-frequency analysis of event-related spectral perturbation (ERSP) for the illusion task. Higher spectral power is found mainly in the frequency range covering the beta (β) band at latencies lower than 100 ms. At 130 ms latency, lower power was activated to cover the relatively low frequency of theta (θ) band or it may reach early alpha (α) band.

Table 1. Summary of the previously reported N1 responses recorded during different illusion tasks. N1 refers to the first negative response appearing after the onset of illusion stimulation, including the grid illusion used in this research.

Illusion type	N1 Component	Finding	Year	Reference
Müller-Lyer illusion task	N170 Parietal Pz	Illusion task elicit more negative ERP deflection than non-illusion stimuli.	2007	[20]
Cue illusion (face or vase)	160 Posterior Pz	The posterior P100 and N160 were elicited only by the face-face and vase-vase responses but not in the opposite of the cue (face-vase or vase-face).	2009	[7]
Rod and Frame Illusion (RFI) orientation illusion	180-200 Over lateral occipital electrodes	P1 and N1 reflect the early visual processing and do not affected with the frame tile of orientation stimulation.	2009	[34]
Abutting line grating illusion contour stimulus	150-200 Over the entire scalp, the peaks earlier over frontal than posterior scalp	The illusion contours could make the occurrence time of N1 came earlier, and the peak became larger.	2012	[33]
Combination of Checkerboard with Scintillating grid illusion	N130 distributed over parietal area in both hemispheres	Evidence to N1 that it might reflect the complex task perception response (puzzled response).	Present	This paper

1) have reported the observation of N1 as a consequence of the illusion task.

However, some other studies have reported the presence of N130 with different types of external stimulation. Halgren *et al.* [35], for example, used emotional visual stimuli and observed the N130 component in the anterior hippocampus and amygdala. Another study [36] indicated the appearance of N130 in posterior scalp with the arithmetic conflict task. With auditory stimulation, it was reported that N130 is not substantially affected by the presence of visual standard stimuli [37]. The presence of N130 was also reported in a recent study [38] on pain perception during electric stimulation. From the above short review (summarized in Table 2) and the current study, we infer that appearance of N130 is affected by visual stimulation but is mostly related to the perceptual process in the brain.

This study provides the first discussion of N130 and its relationship with the puzzled response of the brain. The results show that the response latency and position vary with the change in stimulation task (Fig. 2(a)), as compared to the VEP response recently reported in [39]. Here, changing the stimulation task from standard pattern reversal [39] to the puzzled task causes a delay in the latency, as well as changes in the polarity and scalp location of the brain response. The presence of the N130 response is accentuated in brain perception during puzzled moments. N130 is considered as an early response in the parietal lobe when the subject cannot make a decision in a puzzling. It is also interesting that N130 showed a higher amplitude for the mature group than for the young group, which

is contrary to P100 of VEP [39]. This is a clear indication that N130 is involved in puzzled perception processing.

3.2 Time-frequency analysis

Time-frequency analysis is used to characterize changes or perturbations in the spectral content of EEG data and is considered as a sum of windowed sinusoidal wavelet functions. The mathematical details of this straightforward method are described by Delorme and Makeig [25]. Morlet wavelets are also used to detect transient event-related spectral perturbations (ERSP) in epoched datasets. The Morlet wavelet is a Gaussian windowed sinusoidal wave segment comprising several cycles. A family of wavelets, comprising compressed and stretched versions of the mother wavelet fitting each frequency to be extracted from the EEG, is traditionally constrained to the same number of cycles across frequencies [40].

A wavelet family containing 3 cycles of a sinusoidal oscillation was used here. The wavelet for the 3 Hz frequency spans a time window of 500 ms. Number of cycles in the wavelets used for higher frequencies will continue to expand slowly, reaching half the number of cycles in the equivalent fast Fourier transform window at its highest frequency. This variation in the wavelet from coarser to finer temporal resolution with increasing frequency is achieved at the cost of diminishing frequency resolution as frequency increases.

The mean time-frequency analysis ERSP for the illusion task is shown in Fig. 2(d). Higher spectral power was found mostly in the frequency range covering the beta (β) band (11–32 Hz) at a latency lower than 100 ms. For 130

ms latency, lower power was activated to cover a relatively low frequency band, in the range of 5 to 9 Hz. Thus, the N130 response was detected under the theta (θ) band or it may reach the early alpha (α) band in the parietal area. As the response changed (in latency and scalp locations) following the illusion task compared to VEP, the frequency band expanded to cover the relatively lower frequencies at 130 ms.

No gamma (γ) frequency was noticed in either task, which is consistent with the results of Porcaro *et al.* [41], since this band is related more to the attention process of sensory stimuli and maintenance of working memory, rather than illusion perception. As there was no gamma (γ) frequency related to the illusion task, this supports the previous research stating that the occipital alpha (α) frequency of 10 Hz is the most prominent band related to the functional role of visual perception [42, 43]. The results of the current study are also in agreement with Selimbeyoglu *et al.* [44], who suggest that time-frequency characterization might be useful in the detection of subjective confidence level in decision making. The authors discussed decision difficulty and reported that the frequency band changes with decision accuracy. Decision uncertainty or the puzzled brain response is activated with low frequency bands.

3.3 Cross coherence

The cross coherence between active components were investigated and compared between the different stimulation tasks. As it is well known that the occipital lobe is active in pattern VEP and the current result shows the parietal lobe is active in the illusion

Table 2. Summary of the N130 component characteristics, as reported for different external stimulations. This is the first study to report the presence of N130 in an illusion task.

Stimulation	Task used	Region	Year	Reference
Visual stimulation	Emotional task	Anterior hippocampus and amygdala	1994	[35]
Arithmetic conflict	Arithmetic problem calculation task and matching the result to an answer digit	Posterior scalp areas (occipital and temporal)	2000	[36]
Auditory/visual stimulation	Oddball paradigm	Frontal-central topography; N130 latency shorter at posterior sites than frontal sites	2006	[37]
Electrical stimulations	Pain perception using painful and non-painful task	Frontal /central regions	2014	[38]
Visual illusion stimulation	Grid illusion task count the number of illusion dots	Activation of parietal area	Present	This paper

task, these two lobes were investigated to study coherency between the right and left hemispheres. As shown in Fig. 3, our results show more coherence between the left and right hemispheres of the brain in the illusion task than in pattern VEP.

This is a logical result, since the brain puts forth more effort in identifying an object and its coherency increases with increasing difficulty of identification. As such, the puzzled illusion task will obviously produce larger coherence between brain hemispheres.

3.4 Measure Projection Analysis (MPA)

Scalp channels analysis is a typical practice for investigating and differentiating EEG results across multiple subjects by identifying scalp channels. However, the method is not highly accurate since the channel responses may include non-brain activity within the data. To address this issue, researchers [25] have proposed an ICA algorithm that decomposes the signal into its independent components, which are further clustered and used to extract the brain response. One of the most interesting applications of clustering is localization of the source generator of the brain response through fitting the dipoles of brain components. The most recent method of localization, MPA, was used in this research. MPA statistically characterizes the spatial consistency of EEG dynamics across a set of recorded data by combining the information across a large number of subjects, each associated with his or her own set of source processes and scalp projections [29].

In order to localize the sources of the N130 component resulting from the puzzled task in different age groups, measure projections of relative brain components were utilized. The measure projections with anatomical and functional properties of N130 components are presented in Figs. 4 and 5 for young and mature subjects, respectively. In these figures, the dipole sources were estimated based on the recorded ERP, which were clustered into different domains in the brain subspace. The sources are localized on the MRI image (Figs. 4(a) and Fig. 5(a)), which shows precise brain locations that are comparable to other

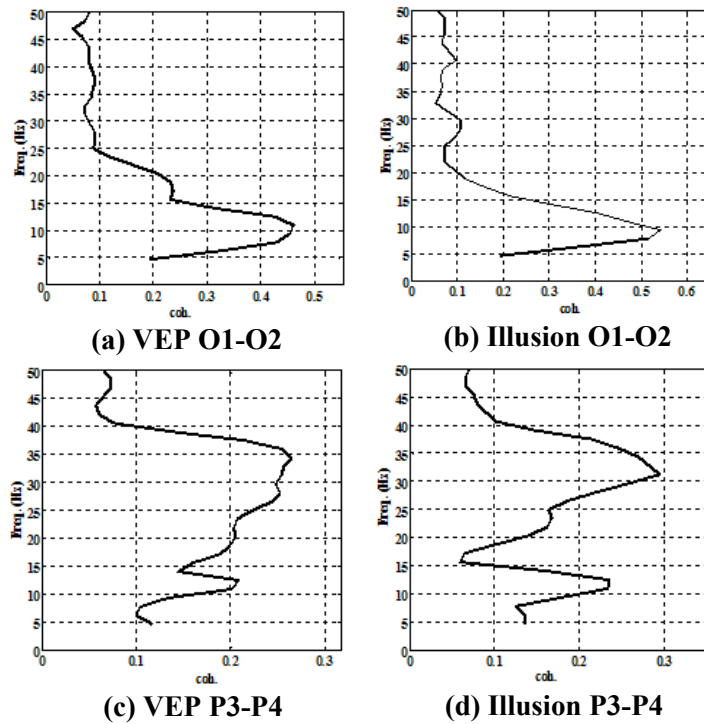


Figure 3. Cross coherence of visual evoked potentials (VEP response as reported in [39]) and illusion between brain hemispheres in the parietal and occipital lobes. Cross coherence increases with the complexity of the task. The puzzled task produces more interaction between brain hemispheres than does VEP.

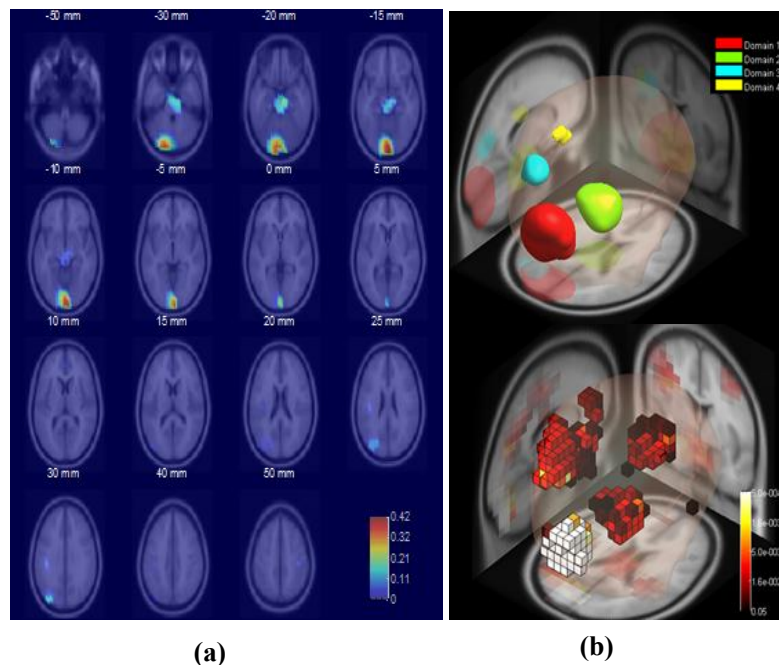


Figure 4. Measure projection analysis of illusion task in the young group. (a) Localization of the sources on the MRI image and (b) clustering of the sources into different domains in the brain subspace. Four domains are estimated. The first domain (domain 1) is in the occipital gyrus, which represents the visual area in the brain. The second domain (domain 2) is projected in the brainstem, which controls involuntary processes. Parts of the third domain (domain 3) and fourth domain (domain 4) are localized in the parietal lobe, forming a multimodal complex region of puzzled sources that include the left angular gyrus, left postcentral gyrus, and left supramarginal gyrus.

studies based on fMRI [5]. The MPA provides a statistically supported, data-driven model of cortical regions exhibiting consistent measure features, and the regions identified may be readily compared to the results of other functional imaging experiments.

The illusion stimulation led to the puzzling task in which the subjects could not make an accurate decision. In presenting the visual stimulation to produce a puzzled perceptual response, activation of the visual area of the brain was expected, and led to marked projections domains in the occipital gyrus. As can be seen clearly in Fig. 4(b), the first main domain and some parts of domain 3 are more or less associated with vision. The primary and secondary visual information in the middle, inferior and superior occipital gyri are projected, as shown in Table 3. The lingual gyrus is also related to vision processing [45]. The lingual gyrus is a brain structure that is especially related to letters and the encoding of visual memories and complex images [45]. A high probability is seen for the cerebellum in domain 1. The cerebellum plays an important role in motor control and may be involved in some cognitive functions such as language and attention, but also in fear regulation and pleasure response [46]. The second domain is projected in the posterior part of brain, close to the brainstem. The brainstem plays an important role in regulating and controlling involuntary processes such as the respiratory, cardiac and sleep cycle functions [45].

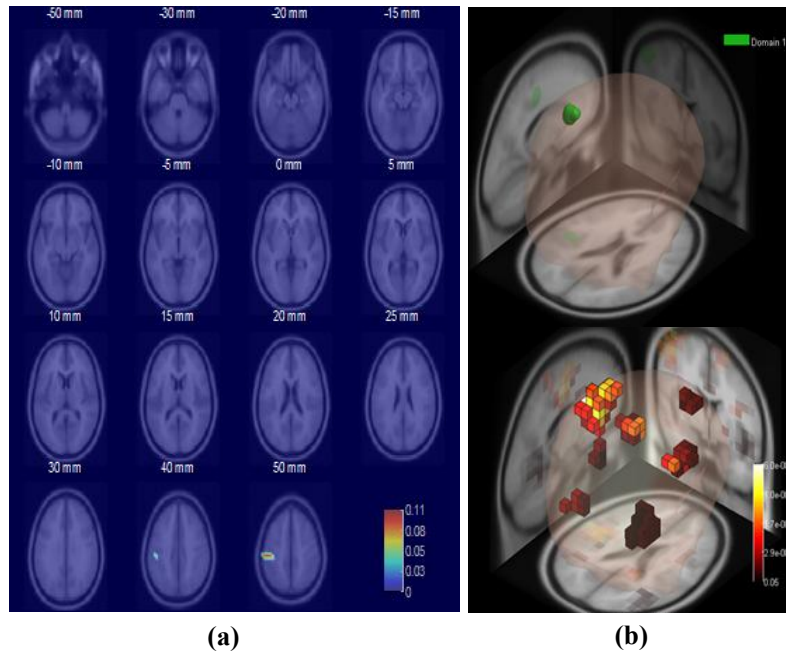


Figure 5. Measure projection analysis of illusion task in the mature age group. (a) Localization of the sources on the MRI image and (b) clustering of the sources into different domains in the brain subspace. One domain (domain 1) is estimated on the multimodal complex region of puzzled sources, which include the left postcentral gyrus, left supramarginal gyrus, and left angular gyrus.

A part of the third domain is located in the angular gyrus (Brodmann’s area 39). The fourth domain is focused on the postcentral gyrus (Brodmann’s areas 3, 1 and 2) and the supramarginal gyrus (Brodmann’s area 40). The same domain is also projected in the illusion task in the mature group, as shown in Fig. 5(b). Since it is the only domain that can be seen in the mature group (as summarized in Table 3), it

likely indicates the sources of N130 related to the puzzled task.

The mature subjects directed their attention to the experimental task (i.e. counting the number of illusory dots), which caused them to ignore other stimuli presented within the task. Therefore, the only domain projected indicates the puzzled source generator in the brain. The young subjects were less able to direct their

Table 3. Measure projection analysis domains’ summary for the illusion task in young and mature subjects. One domain common in both age groups covers the left supra-marginal gyrus, the left postcentral gyrus and the left angular gyrus complex, which represent the source generator of the puzzled response in the brain.

Domain	Projections of illusion task in young group			Projections of illusion task in matured group		
	Anatomical area	Brodmann’s area	Description	Anatomical area	Brodmann’s area	Description
1	Cerebellum	18	Secondary visual (V2)	L Postcentral gyrus	3, 1 and 2 40 39	Primary somatosensory Spatial and semantic processing
	L Inferior occipital gyrus	17	Primary visual (V1)	L Supramarginal gyrus		
	L Lingual gyrus			L Angular gyrus		
2	Brainstem	28	Olfaction	-	-	-
		34				
3	L Middle occipital gyrus	19	Associative visual (V3)	-	-	-
	L Angular gyrus	39	Secondary visual (V2)	-	-	-
	L Superior occipital gyrus	18				
4	L Postcentral gyrus	2	Spatial and semantic processing	-	-	-
	L Supramarginal gyrus	40	Primary somatosensory	-	-	-
		13	Inferior insula			

attention only to the experimental task and therefore, other domains are projected in the analysis.

The angular gyrus is located in the parietal area of the brain that lies superior to the temporal area and immediately posterior to the supramarginal gyrus. It is involved in several brain processes such as number processing and mind theory [47, 48]. The right angular gyrus has been linked to spatiovisual attention toward salient features. For instance, it might play a critical role in distinguishing right and left by integrating the conceptual understanding of the language terms “right” and “left” with its location in space. Since it may be associated with orienting the brains 3-D space, it may also control shifts of attention in space [49, 50].

The primary somatosensory cortex is usually said to be mostly prominent in the parietal lobe and is associated with the postcentral gyrus, where it is involved in sensations such as touch [51]. The supramarginal gyrus is a portion of the parietal lobe located in Brodmann’s area 40, which participates in language perception and lexical-semantic processing. Both the right and left supramarginal gyri activate when phonological word choices are made. A portion of the supramarginal gyrus appears

to play a central role in controlling empathy or very quick judgments (quick decisions) [52]. Together, the supramarginal and angular gyri constitute a multimodal associative area that is activated when words are linked with their meanings. As the supramarginal gyrus is located just dorsal to the angular gyrus, these two structures form a multimodal complex that receives somatosensory, visual and auditory inputs from the brain. The current results indicate that in addition to body sensations, the left supramarginal gyrus, left postcentral gyrus, and left angular gyrus form a multimodal complex region that might be responsible for generating the response to complex tasks related to untrusted decisions, including the puzzled response.

4. Conclusion

This study compared brain responses to the puzzled task, brain topography time-frequency analysis, cross coherency and source fitting dipole localization. The puzzled task presented a negative response at 130 ms with frequency of theta (θ) band, or it may reach early alpha (α) band (5-9 Hz) in the parietal lobe since it is activated at a lower frequency

band than VEP. Cross coherence increased with the complexity of the task, and the puzzled task produced more interaction between the hemispheres of the brain. An age-related comparison revealed a significant difference in N130 amplitude and a slight difference in the source generator of the puzzled component, which could reflect the maturity level of the brain. Puzzled task sources were estimated to consist of a complex multimodal region that comprises the left postcentral gyrus, supramarginal gyrus and angular gyrus. This study introduces descriptions of the brain perceptions evoked by the puzzled task when the brain is unresponsive to the task. It provides evidence of the brain component N130’s association with puzzled perception.

Acknowledgments

Conflict of interest statement: We have no conflict of interest to declare. The authors would like to thank the Department of Physics Faculty of Science, Universiti Teknologi Malaysia, for their financial support. This research was supported by Research University Grant (GUP/MOHE), Vot Number: QJ130000.2526.07H93.

References

- [1] Greimel E., Trinkl M., Bartling J., Bakos S., Grossheinrich N., Schulte-Koerne G., Auditory selective attention in adolescents with major depression: an event-related potential study, *J. Affect. Disord.*, 2015, 172, 445-452
- [2] Gherman S., Philiastides M. G., Neural representations of confidence emerge from the process of decision formation during perceptual choices, *Neuroimage*, 2015, 106, 134-143
- [3] Philiastides M. G., Sajda P., Temporal characterization of the neural correlates of perceptual decision making in the human brain, *Cereb. Cortex*, 2006, 16, 509-518
- [4] Philiastides M. G., Ratcliff R., Sajda P., Neural representation of task difficulty and decision making during perceptual categorization: a timing diagram, *J. Neurosci.*, 2006, 26, 8965-8975
- [5] Philiastides M. G., Sajda P., EEG-informed fMRI reveals spatiotemporal characteristics of perceptual decision making, *J. Neurosci.*, 2007, 27, 13082-13091
- [6] Sulykos I., Czigler I., Visual mismatch negativity is sensitive to illusory brightness changes, *Brain Res.*, 2014, 1561, 48-59
- [7] Qiu J., Wei D. T., Li H., Yu C. Y., Wang T., Zhang Q. L., The vase-face illusion seen by the brain: an event-related brain potentials study, *Int. J. Psychophysiol.*, 2009, 74, 69-73
- [8] Boutsen L., Humphreys G. W., Praamstra P., Warbrick T., Comparing neural correlates of configural processing in faces and objects: an ERP study of the Thatcher illusion, *Neuroimage*, 2006, 32, 352-367
- [9] Gu X., Yang X., Zhu Y., Spatial-temporal analysis of face processing using an ERP study of the Thatcher illusion, *Conf. Proc. IEEE Eng. Med. Biol. Soc.*, 2007, 2496-2499
- [10] Kuefner D., Jacques C., Prieto E. A., Rossion B., Electrophysiological correlates of the composite face illusion: disentangling perceptual and decisional components of holistic face processing in the human brain, *Brain Cogn.*, 2010, 74, 225-238
- [11] Niedeggen M., Heil M., Ludwig E., Rolke B., Harris C. L., Priming illusory words: an ERP approach, *Neuropsychologia*, 2004, 42, 745-753
- [12] Chow W. Y., Phillips C., No semantic illusions in the “Semantic P600” phenomenon: ERP evidence from Mandarin Chinese, *Brain Res.*, 2013, 1506, 76-93
- [13] Tune S., Schlesewsky M., Small S. L., Sanford A. J., Bohan J., Sassenhagen J., et al., Cross-linguistic variation in the neurophysiological response to semantic processing: evidence from anomalies at the borderline of awareness, *Neuropsychologia*, 2014, 56, 147-166
- [14] Halgren E., Mendola J., Chong C. D. R., Dale A. M., Cortical activation

- to illusory shapes as measured with magnetoencephalography, *Neuroimage*, 2003, 18, 1001-1009
- [15] Bakhtazad L., Shumikhina S., Molotchnikoff S., Analysis of frequency components of cortical potentials evoked by progressive misalignment off Kanizsa squares, *Int. J. Psychophysiol.*, 2003, 50, 189-203
- [16] Senkowski D., Rottger S., Grimm S., Foxe J. J., Herrmann C. S., Kanizsa subjective figures capture visual spatial attention: evidence from electrophysiological and behavioral data, *Neuropsychologia*, 2005, 43, 872-886
- [17] Brown C., Gruber T., Boucher J., Rippon G., Brock J., Gamma abnormalities during perception of illusory figures in autism, *Cortex*, 2005, 41, 364-376
- [18] Sokhadze E. M., El-Baz A., Baruth J., Mathai G., Sears L., Casanova M. F., Effects of low frequency repetitive transcranial magnetic stimulation (rTMS) on gamma frequency oscillations and event-related potentials during processing of illusory figures in autism, *J. Autism Dev. Disord.*, 2009, 39, 619-634
- [19] Stroganova T. A., Orekhova E. V., Prokofyev A. O., Tsetlin M. M., Gratchev V. V., Morozov A. A., et al., High-frequency oscillatory response to illusory contour in typically developing boys and boys with autism spectrum disorders, *Cortex*, 2012, 48, 701-717
- [20] Qiu J., Li H., Zhang Q. L., Liu Q., Zhang F. H., The Müller-Lyer illusion seen by the brain: An event-related brain potentials study, *Biol. Psychol.*, 2008, 77, 150-158
- [21] Saint-Amour D., De Sanctis P., Molholm S., Ritter W., Foxe J. J., Seeing voices: high-density electrical mapping and source-analysis of the multisensory mismatch negativity evoked during the McGurk illusion, *Neuropsychologia*, 2007, 45, 587-597
- [22] Van den Bos R., Den Heijer E., Vlaar S., Houx B., Exploring gender differences in decision-making using the Iowa Gambling Task, Murphy D., Longo D. (Eds.) *Encyclopedia of psychology of decision making*, Nova Science Publishers, New York, NY, USA, 2007, 1115
- [23] Odom J. V., Bach M., Brigell M., Holder G. E., McCulloch D. L., Tormene A. P., et al., ISCEV standard for clinical visual evoked potentials (2009 update), *Doc. Ophthalmol.*, 2009, 120, 111-119
- [24] Geier J., Bernáth L., Hudák M., Séra L., Straightness as the main factor of the Hermann grid illusion, *Perception*, 2008, 37, 651-665
- [25] Delorme A., Makeig S., EEGLAB: an open source toolbox for analysis of single-trial EEG dynamics including independent component analysis, *J. Neurosci. Meth.*, 2004, 134, 9-21
- [26] Le Van Quyen M., Foucher J., Lachaux J. P., Rodriguez E., Lutz A., Martinerie J., et al., Comparison of Hilbert transform and wavelet methods for the analysis of neuronal synchrony, *J. Neurosci. Meth.*, 2001, 111, 83-98
- [27] Schack B., Vath N., Petsche H., Geissler H. G., Moller E., Phase-coupling of theta-gamma EEG rhythms during short-term memory processing, *Int. J. Psychophysiol.*, 2002, 44, 143-163
- [28] Schack B., Klimesch W., Sauseng P., Phase synchronization between theta and upper alpha oscillations in a working memory task, *Int. J. Psychophysiol.*, 2005, 57, 105-114
- [29] Bigdely-Shamlo N., Mullen T., Kreutz-Delgado K., Makeig S., Measure projection analysis: a probabilistic approach to EEG source comparison and multi-subject inference, *Neuroimage*, 2013, 72, 287-303
- [30] Bigdely-Shamlo N., Vankov A., Ramirez R. R., Makeig S., Brain activity-based image classification from rapid serial visual presentation, *IEEE Trans. Neural Syst. Rehabil. Eng.*, 2008, 16, 432-441
- [31] Bell A. J., Sejnowski T. J., The "independent components" of natural scenes are edge filters, *Vision Res.*, 1997, 37, 3327-3338
- [32] Wascher E., Hoffmann S., Sängler J., Grosjean M., Visuo-spatial processing and the N1 component of the ERP, *Psychophysiology*, 2009, 46, 1270-1277
- [33] Todo Y., Chen W., Tang H., Visual illusion and N1 and P1: ERP evidence, *Int. J. Appl. Sci. Tech.*, 2012, 2, 8-13
- [34] Corbett J. E., Enns J. T., Handy T. C., Electrophysiological evidence for a post-perceptual influence of global visual context on perceived orientation, *Brain Res.*, 2009, 1292, 82-92
- [35] Halgren E., Baudena P., Heit G., Clarke M., Marinkovic K., Spatio-temporal stages in face and word processing. 1. Depth recorded potentials in the human occipital and parietal lobes, *J. Physiol.*, 1994, 88, 1-50
- [36] Wang Y. P., Kong J., Tang X. F., Zhuang D., Li S. W., Event-related potential N270 is elicited by mental conflict processing in human brain, *Neurosci. Lett.*, 2000, 293, 17-20
- [37] Brown C. R., Clarke A. R., Barry R. J., Inter-modal attention: ERPs to auditory targets in an inter-modal oddball task, *Int. J. Psychophysiol.*, 2006, 62, 77-86
- [38] Wang C. B., Ma Y. N., Han S. H., Self-construal priming modulates pain perception: event-related potential evidence, *Cogn. Neurosci.*, 2014, 5, 3-9
- [39] Almurshedi A., Ismail A. K., Measure projection analysis of VEP localization neuron generator, *Conf. Proc. IEEE Eng. Med. Biol. Soc.*, 2015, in press, DOI: 978-1-4799-6879-4/15
- [40] Roach B. J., Mathalon D. H., Event-related EEG time-frequency analysis: an overview of measures and an analysis of early gamma band phase locking in schizophrenia, *Schizophr. Bull.*, 2008, 34, 907-926
- [41] Porcaro C., Ostwald D., Hadjipapas A., Barnes G. R., Bagshaw A. P., The relationship between the visual evoked potential and the gamma band investigated by blind and semi-blind methods, *Neuroimage*, 2011, 56, 1059-1071
- [42] Palva S., Palva J. M., New vistas for alpha-frequency band oscillations, *Trends Neurosci.*, 2007, 30, 150-158
- [43] VanRullen R., Macdonald J. S. P., Perceptual echoes at 10 Hz in the human brain, *Curr. Biol.*, 2012, 22, 995-999
- [44] Selimbeyoglu A., Keskin-Ergen Y., Demiralp T., What if you are not sure? Electroencephalographic correlates of subjective confidence level about a decision, *Clin. Neurophysiol.*, 2012, 123, 1158-1167
- [45] Carter R., *The brain book*, Dorling Kindersley, London, UK, 2009
- [46] Wolf U., Rapoport M. J., Schweizer T. A., Evaluating the affective component of the cerebellar cognitive affective syndrome, *J.*

Neuropsychiatry Clin. Neurosci., 2009, 21, 245-253

- [47] Grabner R. H., Ansari D., Reishofer G., Stern E., Ebner F., Neuper C., Individual differences in mathematical competence predict parietal brain activation during mental calculation, *Neuroimage*, 2007, 38, 346-356
- [48] Arsalidou M., Taylor M. J., Is $2+2=4$? Meta-analyses of brain areas needed for numbers and calculations, *Neuroimage*, 2011, 54, 2382-2393
- [49] Seghier M. L., The angular gyrus: multiple functions and multiple subdivisions, *Neuroscientist*, 2013, 19, 43-61
- [50] Chen Q., Weidner R., Vossel S., Weiss P. H., Fink G. R., Neural mechanisms of attentional reorienting in three-dimensional space, *J. Neurosci.*, 2012, 32, 13352-13362
- [51] Eickhoff S. B., Schleicher A., Zilles K., Amunts K., The human parietal operculum. I. Cytoarchitectonic mapping of subdivisions, *Cereb. Cortex*, 2006, 16, 254-267
- [52] Hartwigsen G., Baumgaertner A., Price C. J., Koehnke M., Ulmer S., Siebner H. R., Phonological decisions require both the left and right supramarginal gyri, *Proc. Natl. Acad. Sci. USA*, 2010, 107, 16494-16499